of 10, 25 and 50 kGy were respectively 195,000, 142,000 and 95,000 by GPC.

Micromass Culture of Osteoblasts. Mouse osteoblast-like MC3T3-E1 cells (RIKEN Cell Bank, Japan) and normal human osteoblast NHOst cells (Clonetics Corporation, MD, USA) were grown in alpha minimum essential medium (α-MEM) supplemented with 20% fetal bovine serum. The PLLA sheet was cut into 14.0 mm diameter disk and laid in a 24-well dish. The 20 μl of cell suspension (2×10^6 cells/ml) was delivered on the disk. After the cells were attached on the disk, 1 ml of the complete medium that contained 10 mM disodium β-glycerophosphate in the culture medium was added. The complete medium was changed three times a week, and the cells cultured for 2 weeks in a 37°C humidified atmosphere of 5% CO_2.

Proliferation Assay. The number of the cells cultured on the PLLA sheet was determined by WST-8 assay [5]. Moreover, the protein and DNA contents of the cell lysate were measured by the Lowry method and the fluorescence assay using Hoechst 33258 dye, respectively [5].

Differentiation Assay. The calcium depositions of the cell cultures were stained by alizarin red S, and the areas stained dark-red were measured using the program Scion Image (Scion Co., MD, USA) [5]. The calcification was calculated as the normalized area in the cell number. Moreover, the collagen synthesis was evaluated by the hydroxyproline content of the cell lysate, and ALP activity of the cells was measured using *p*-nitrophenylphosphate as a substrate [5].

Soaking in the Medium. The PLLA sheet was cut into 14.0 mm diameter disk and laid in a 24-well dish. The complete medium of 1 ml was added without the cells. Then, the dish was stored in a 37°C humidified atmosphere of 5% CO_2, and the complete medium was changed three times a week. After soaking for 2 weeks, the PLLA disk was washed in deionized water five times quickly and dried in a silica gel desiccator.

Surface Analysis. The surface of the PLLA sheet after soaking in the complete medium without the cells was characterized by SEM, EDX, FT-IR and XPS according to the conventional methods.

Results

Proliferation of Osteoblasts Cultured on the PLLA Sheet. The cell number of MC3T3-E1 cells cultured on the PLLA sheet did not change with increasing irradiation dose (Fig. 1a). The protein and DNA contents of the cells also did not change. The other side, the cell number (Fig. 1b),

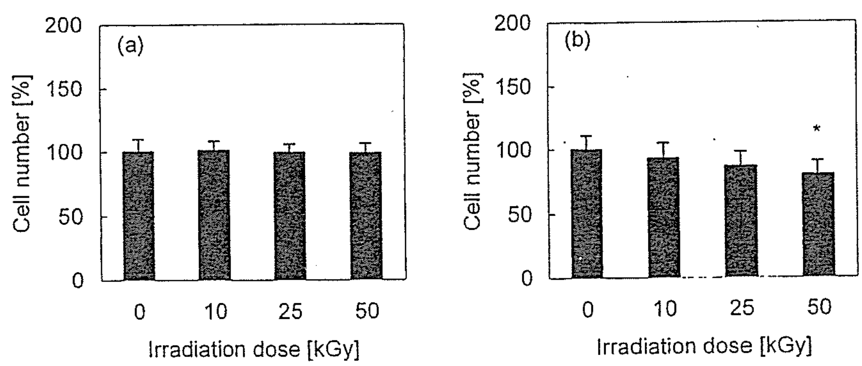

Fig. 1. The cell numbers of (a) MC3T3-E1 and (b) NHOst cells cultured on the γ-irradiated PLLA sheet.

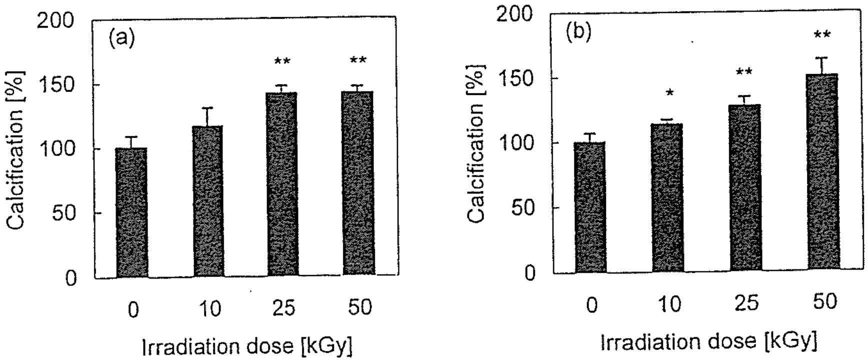

Fig. 2. The calcifications of (a) MC3T3-E1 and (b) NHOst cells cultured on the γ-irradiated PLLA sheet.

protein and DNA contents of NHOst cells cultured on the PLLA sheet slightly decreased with irradiation dose.

Differentiation of Osteoblasts Cultured on the PLLA Sheet. The calcification of MC3T3-E1 cells (Fig. 2a) and NHOst cells (Fig. 2b) remarkably increased with irradiation dose. The collagen synthesis and ALP activity of MC3T3-E1 and NHOst cells also increased as same as the calcification, respectively. The γ-irradiated PLLA remarkably promoted the differentiation of osteoblasts.

Apatite Formation on the PLLA Sheet. The SEM micrograph exhibited crystal particles on the surface of the PLLA sheet after soaking in the complete medium without the cells. The crystal particles were identified with hydroxyapatite by EDX, FT-IR and XPS spectra. The phosphate band in ATR/FT-IR spectra became strong with irradiation dose (Fig. 3). Moreover, the element rations of calcium and phosphorus increased but that of carbon decreased with irradiation dose, in XPS analysis (Fig. 4). The amount of hydroxyapatite formed on the γ-irradiated PLLA sheet increased with irradiation dose.

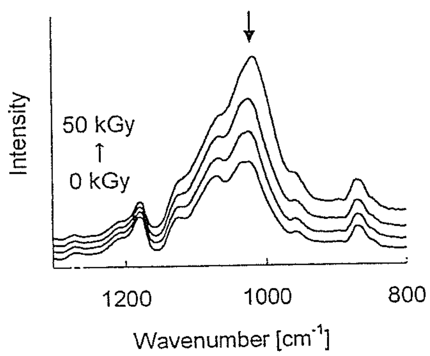

Fig. 3. The phosphate band of the γ-irradiated PLLA sheet after soaking in the medium.

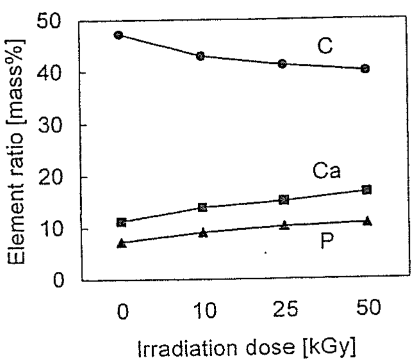

Fig. 4. The element ratios of calcium, phosphorus and carbon of the γ-irradiated PLLA sheet after soaking in the medium.

Discussion

In the present study, the γ-irradiated PLLA hardly affected the proliferation but remarkably promoted the differentiation of osteoblasts. It was expected that the low molecular weight PLLA eluted to the medium, because the molecular weight of PLLA decreased by γ-irradiation. In our recent studies, the low molecular weight PLLA enhanced the differentiation of MC3T3-E1 cells but inhibited that of NHOst cells [6, 7]. The present results, which the differentiations of MC3T3-E1 and NHOst cells both increased on the γ-irradiated PLLA sheet, would not be caused by the low molecular weight PLLA. The surface of the γ-irradiated PLLA should good influence on the differentiation of osteoblasts.

On the other hand, the γ-irradiation increased the apatite-forming ability of the PLLA sheet. Tanahashi and Matsuda reported that some negatively charged groups such as phosphate and carboxyl group strongly induced apatite formation in a simulated body fluid. They described that the apatite formation was initiated via calcium ion-absorption upon complexation with a negative surface-charged group [8]. In our study, the molecular weight of PLLA decreased with hydrolysis of ester bonds by γ-irradiation [2]. Therefore, the amount of carboxyl group of the γ-irradiated PLLA would increase with irradiation dose, and the carboxyl group would promote the apatite-forming ability of the PLLA sheet.

Fujibayashi *et al.* compared *in vivo* bone ingrowth and *in vitro* apatite formation on Na_2O-CaO-SiO_2 glasses. The quantities of newly bone formed on the glasses correlated with their apatite-forming abilities in simulated body fluid. They propose to evaluate the apatite-forming ability in order to confirm the *in vivo* bioactibity of biomaterials [9]. In our present study, the γ-irradiation enhanced the apatite-forming ability of the PLLA sheet, and then the γ-irradiated PLLA sheet promoted the differentiation of osteoblasts. The osteoblast differentiation should connect with the apatite formation on the γ-irradiated PLLA sheet.

In conclusion, the γ-irradiated PLLA hardly affected the proliferation but promoted the differentiation of osteoblasts with increasing irradiation dose. On the other hand, the hydroxyapatite was formed on the PLLA sheet in the medium, and the γ-irradiation enhanced apatite-forming ability of the PLLA. It was suggested that the connection between the osteoblast differentiation and apatite formation on the γ-irradiated PLLA sheets.

References

[1] T.E. Otto, P. Patka, H.J.Th.M. Haarman, C.P.A.T. Klein and R. Vriesde: J. Mater. Sci. Mater. Med. 5 (1994), 407-410.

[2] K. Isama and T. Tsuchiya: Bull. Natl. Inst. Health Sci. 119 (2001), 61-64.

[3] X. Yuan, A.F.T. Mak and J. Li: J. Biomed. Mater. Res. 57 (2001), 140-150.

[4] N. Olmo, A.I. Martin, A.J. Salinas, J. Turnay, M. Vallet-Regi and M.A. Lizarbe: Biomaterials 24 (2003), 3383-3393.

[5] K. Isama and T. Tsuchiya: J. Biomater. Sci. Polymer Edn. 13 (2002), 153-166.

[6] K. Isama and T. Tsuchiya: Biomaterials 24 (2003), 3303-3309.

[7] K. Isama, Y. Ikarashi and T. Tsuchiya: BIO INDUSTRY 19 (2002), 21-29.

[8] M. Tanahashi and T. Matsuda: J. Biomed. Mater. Res. 34 (1997), 305-315.

[9] S. Fujibayashi, M. Neo, H.M. Kim, T. Kokubo and T. Nakamura: Biomaterials 24 (2003), 1349-1356.

Available online at www.sciencedirect.com
SCIENCE DIRECT
Biomaterials 26 (2005) 5138–5144
Biomaterials
www.elsevier.com/locate/biomaterials

The response of normal human osteoblasts to anionic polysaccharide polyelectrolyte complexes

Misao Nagahata[a,b,1], Ryusuke Nakaoka[a,1,*], Akira Teramoto[b], Koji Abe[b], Toshie Tsuchiya[a]

[a]Division of Medical Devices, National Institute of Health Sciences, 1-81-1 Kamiyoga, Setagaya-ku, Tokyo 158-8501, Japan
[b]Department of Functional Polymer Science, Faculty of Textile Science and Technology, Shinshu University, Ueda 386-8567, Japan

Received 10 September 2004; accepted 7 January 2005

Abstract

Polyelectrolyte complexes (PEC) were prepared from chitosan as the polycation and several synthesized functional anion polysaccharides, and their effects on cell attachment, morphology, proliferation and differentiation were estimated using normal human osteoblasts (NHOst). After a 1-week incubation, PEC made from polysaccharides having carboxyl groups as polyanions showed low viability of NHOst on it although the NHOst on it showed an enhancement in their differentiation level. On the other hand, NHOst on PEC made from sulfated or phosphated polysaccharides showed similar attachment and morphology to those on the collagen-coated dish. When the number of NHOst was estimated after 1 week, the number on the PEC was ranged from 70% to 130% of those on the collagen-coated dish, indicating few effects of these PEC on cell proliferation. In addition, NHOst on PEC films made from sulfated polysaccharides differentiated to a level very similar to that observed on the collagen-coated dish, indicating that these PEC films maintain the normal potential of NHOst to both proliferate and differentiate. Measurement of gap junctional intercellular communication of NHOst on PEC revealed that PEC did not inhibit communication, suggesting that PEC films have few effects on cell homeostasis. Thus, PEC made from the sulfated polysaccharide may be a useful material as a new scaffold for bone regeneration.

Keywords: Polyelectrolyte complex; Normal human osteoblasts; Cell proliferation; Cell differentiation; Gap junctional intercellular communication

1. Introduction

The extracellular matrix (ECM) provides an essential three-dimensional (3D) environment for cells to construct several kinds of tissues. The ECM, consisting of numerous kinds of molecules such as proteins, polysaccharides and proteoglycans regulates the behavior of surrounding cells to form tissues and organs precisely [1,2]. For tissue regeneration trials using in vitro techniques, therefore, it is indispensable to develop a synthetic ECM scaffold that functions similarly to the native ECM. For more than a decade, engineering of new tissues by using selective cell transplantation on polymer scaffolds as an artificial ECM instead of tissue transplantation to other living bodies has been studied [3,4]. Recently, many studies on developing a scaffold for tissue regeneration have been done using ECM proteins such as collagen and gelatin [5–7], biodegradable synthetic polymers [8–10] and polysaccharides [11,12]. Because proteins derived from human tissues have many problems such as antigenicity or potential for infection, a biocompatible synthetic polymer or polysaccharide may be preferable for tissue regeneration.

*Corresponding author. Division of Medical Devices, National Institute of Health Sciences, 1-18-1 Kamiyoga, Setagaya-ku, Tokyo 158-8501, Japan. Tel.: +81 3 3700 9264; fax: +81 3 3707 6950.
E-mail addresses: nagahata@nihs.go.jp (M. Nagahata), nakaoka@nihs.go.jp (R. Nakaoka).
[1]These authors contributed equally to this work.

0142-9612/$ - see front matter © 2005 Elsevier Ltd. All rights reserved.
doi:10.1016/j.biomaterials.2005.01.041

A polyelectrolyte complex (PEC) is a compound made from an electrically neutralized molecular complex of polyanions and polycations [13]. PEC can be prepared in various forms such as a film (2D) and a hydrogel, a microcapsule or a sponge (3D), which can be used as a scaffold in tissue regeneration studies. The effects of PEC films composed of polysaccharides on cell behavior have been studied, and we have already reported that PEC can stimulate differentiation of osteoblasts and periodontal ligament fibroblasts [14–16]. These studies suggest that PEC can be used as a biomaterial for repairing or regenerating tissues. In addition, because the PEC are composed of polysaccharides, PEC is expected not to elicit immune responses against it and to have better biocompatibility with the human body, although this is yet to be proved. Therefore, it is necessary to study the interactions between PEC and cells, especially human-derived, to clarify the usefulness of PEC as a biomaterial.

In this study, normal human osteoblasts (NHOst) were cultured on various PEC prepared on a tissue culture plate from chitosan as the polycation and modified chitins or hyaluronan as the polyanion. It should be generally agreed that estimating not only functional advantages but also safety and biocompatibility of biomaterials is important to develop them for clinical use, but the latter is not always studied. Therefore, we measured changes in gap junctional intercellular communication (GJIC) as well as the cell number and differentiation. GJIC is very important function for almost all cells to maintain their homeostasis [17]. During this decade, we have studied the effects of model biomaterials on the GJIC of cells cultured on them and suggested a possibility that changes in the GJIC can be used as an index of biocompatibility of biomaterials [18–21]. Therefore, we measured changes in GJIC of NHOst on PEC in order to estimate the biocompatibility of PEC from their effects on these cell functions.

2. Materials and methods

2.1. Chemicals

Fig. 1 shows the chemical structures of the polyanions and the polycation. Chitosan as the cationic polysaccharide and carboxymethylated chitin [CM-Chitin: degree of substitution (DS) = 1.0 (1.0 anionic site/saccharide ring)] were purchased from Katokichi Co., Ltd. (Kagawa, Japan). Sulfated chitin (S-Chitin: DS = 1.5), phosphated chitin (P-Chitin: DS = 1.6), hyaluronan (HA), and sulfated hyaluronan (SHA: DS = 1.05) were prepared as previously reported [14–16,22].

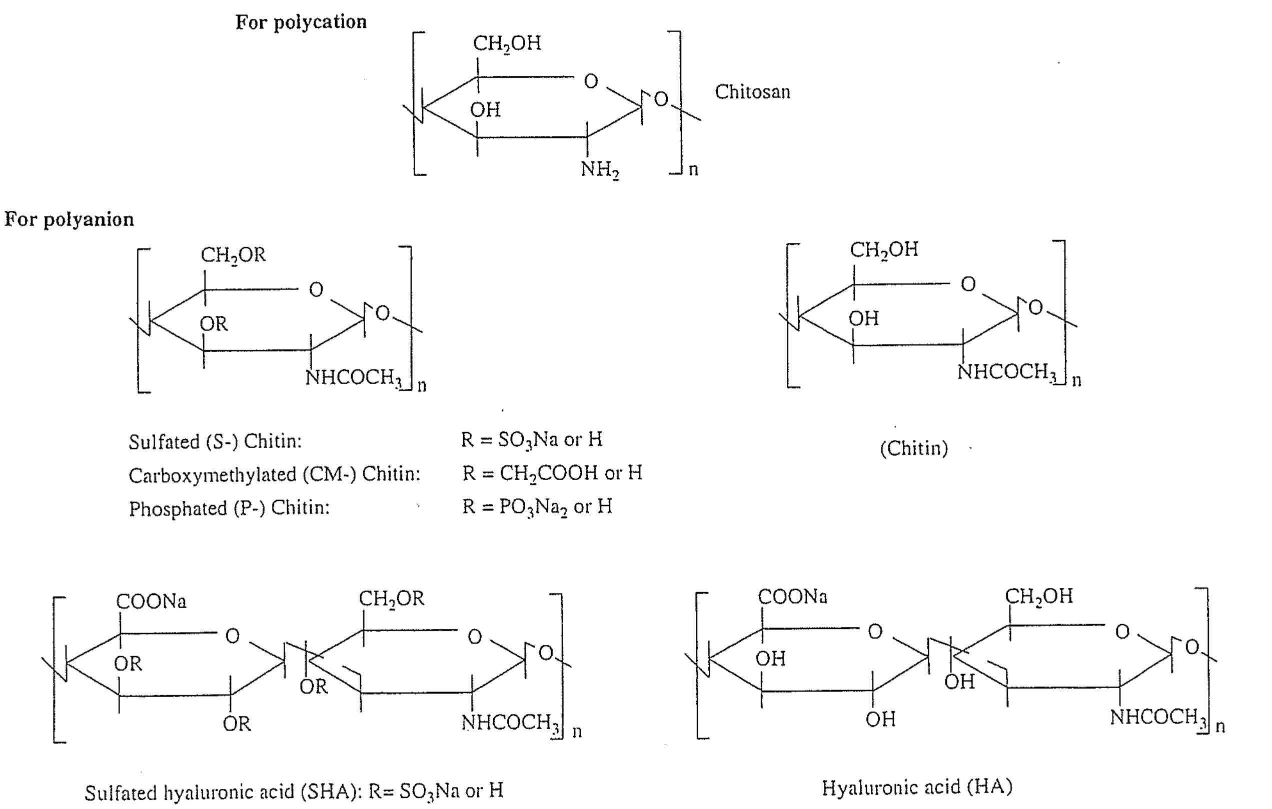

Fig. 1. Polymers for polyelectrolyte complex (PEC) in this study.

2.2. Preparation of PEC and PEC-coated dishes

Polyanions were dissolved individually in distilled water (final concentration = 5×10^{-4} mol of ionic sites/l), and the pH of the solutions was adjusted to 7.4 by adding aqueous HCl or NaOH. Chitosan was dissolved in aqueous 0.5% acetic acid solution and the pH adjusted to 6.0. The ratio of the solutions of polyanions and polycation was adjusted in each combination to neutralize the charge balance of PEC. This mixed solution (1 ml/35 mm tissue culture dish) was allowed to stand overnight at room temperature. After removing the supernatant solution, the dish was dried and annealed at 65 °C in an oven. Then, the dishes were washed with distilled water and oven-dried again to form the PEC-coated dish. This dish was sterilized for 3 min in a microwave oven. Water contact angles of PEC films were measured with the sessile drop method [23], and their zeta potentials were measured by Otsuka Electronics Co., Ltd. (Osaka, Japan).

2.3. Cell culture

NHOst were purchased from BioWhittaker Inc. (Walkersville, MD). The standard culture of NHOst was performed using alpha minimum essential medium (Gibco, Grand Island, NY) containing 20% fetal calf serum (FCS) (Kokusai Shiyaku Co., Ltd., Tokyo Japan). The cells were maintained in incubators under standard conditions (37 °C, 5%-CO_2–95%-air, saturated humidity). All assays were performed using alpha minimum essential medium containing 20% FCS, supplemented with 10 mM beta-glycerophosphate. NHOst cells (1×10^5 cells/dish/2.5 ml medium) were cultured on PEC-coated dishes to evaluate the effects of their interaction with PEC. In each experiment, the medium was changed three times before GJIC of the cells was measured and their differentiation level was evaluated after a 1-week incubation.

2.4. Estimation of differentiation level of NHOst cultured on PEC films

The proliferation of NHOst cells cultured on PEC films was estimated by Tetracolor One assay (Seikagaku Co., Tokyo, Japan), which incorporates an oxidation-reduction indicator based on detection of metabolic activity. After a 1-week incubation, 20 µl of Tetracolor One solution was added to each test dish, followed by a further 2 h incubation. The absorbance of the supernatant at 450 nm was estimated by µQuant spectrophotometer (Bio-tek Instruments, Inc., Winooski, VT). Estimation of alkaline phosphatase (ALP) activity was performed according to an original procedure by Ohyama et al. [24]. After estimating the proliferation of the NHOst cells cultured on PEC films, the cells were washed by phosphate-buffered saline (PBS(−)), followed by addition of 1 ml of 0.1 M glycine buffer (pH 10.5) containing 10 mM $MgCl_2$, 0.1 mM $ZnCl_2$ and 4 mM *p*-nitrophenylphosphate sodium salt. After incubating the cells at room temperature for 7 min, the absorbance of the glycine buffer was detected at 405 nm using µQuant to evaluate the ALP activity of the test cells. The amounts of calcium deposited by the cell during a 1-week incubation were evaluated as follows: after fixing the cells in PBS(−) containing 3% formaldehyde and washing the cells with PBS(−), 0.5 ml of 0.1 M HCl was added to each well. The amounts of calcium dissolved in HCl were estimated using a calcium detecting kit (Calcium-C test Wako, Wako, Osaka, Japan) according to manufacturer's instruction.

2.5. Measurements of GJIC activity

NHOst cultured on PEC films were subjected to fluorescence recovery after photobleaching (FRAP) analysis to estimate the inhibitory activity of these films on the GJIC. FRAP analysis was carried out according to the procedure of Wade et al. [25] with some modifications [21]. Briefly, NHOst were plated on PEC-coated dishes and incubated for 1 or 7 days. The cells were incubated for 5 min at room temperature in PBS(−) containing Ca^{2+} and Mg^{2+} (PBS(+)) and a fluorescent dye, 5,6-carboxyfluorescein diacetate. After washing off excess extracellular dye with PBS(+), the cells in PBS(+) contacting at least two other cells were subjected to FRAP analysis under a Ultima-Z confocal microscope (Meridian Instruments, Okemos, MI) with a 10 × objective lens at room temperature. The cells were photobleached with a 488 nm beam, and recovery of fluorescence intensity was subsequently monitored at 1-min intervals for a total of 4 min. The data obtained from more than seven independent cells were expressed as the average ratio of the fluorescence recovery rate to the rate obtained from NHOst cultured on a collagen-coated dish.

2.6. Statistic analysis

All data were expressed as mean values ± standard deviation of the obtained data. The Fisher–Tukey criterion was used to control for multiple comparisons and to compute the least significant difference between means.

3. Results and discussion

When NHOst were cultured on five kinds of PEC films, their morphology and attachment to the film differed with the composition of the PEC. Fig. 2 shows the morphologies of the NHOst adhering to PEC films.

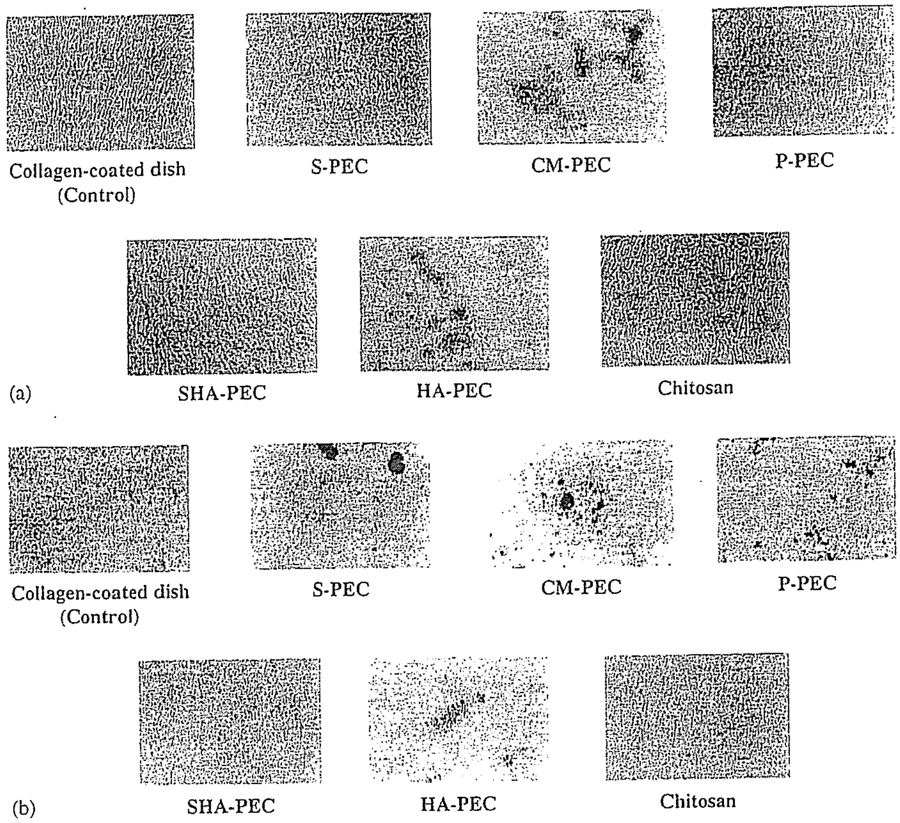

Fig. 2. Light micrographs of normal human osteoblasts (NHOst) on various PEC films after a 2-day incubation: (a) and 1-week incubation, (b). (Original magnification: × 100).

After 2-day incubation, the NHOst on PEC composed of chitosan and either sulfated chitin (S-PEC) or sulfated hyaluronan (SHA-PEC) showed morphologies similar to those on a normal culture plate. When cells were cultured on PEC of chitosan and phosphated chitin (P-PEC), some of them formed small aggregates, while the rest showed morphologies similar to those on S-PEC and SHA-PEC. On the other hand, NHOst cultured on PEC from chitosan and either carboxymethyl chitin (CM-PEC) or hyaluronan (HA-PEC) did not adhere well and showed aggregation. Similar morphologies of the cells on the PEC were observed after 1 day of incubation (data not shown). Even after 1 week of incubation, the morphologies and attachment of the cells on the PEC films did not change (Fig. 2). Only cells grown on cationic polysaccharide chitosan-coated culture dishes preserved morphology of very similar to NHOst grown on collagen-coated cultured dishes, indicating that these morphological differences are ascribable to differences in the anionic polysaccharides of which the PEC is composed.

It has been reported that cell attachment, morphology, and response are influenced by physico-chemical properties of the material surface [23,26]. To clarify what properties of PEC control the attachment and morphology of the cell, the contact angle and zeta potential of PEC films were estimated. Although their compositions are different, large differences in their contact angles were not observed (Fig. 3). On the other hand, a measurement of zeta potentials of the PEC showed interesting results (Table 1). The measurement revealed that S-PEC and SHA-PEC have negative zeta potentials, whereas PEC films made of polysaccharides

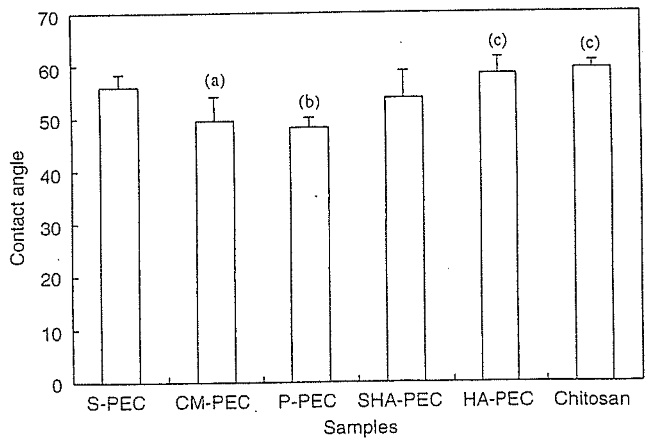

Fig. 3. Contact angles of PEC films studied: (a) $p<0.05$ against S-PEC, (b) $p<0.01$ against S-PEC, (c) $p<0.01$ against both CM-PEC and P-PEC.

Table 1
Zeta potentials of various PEC prepared on a culture dish

	Culture	S-PEC	CM-PEC	P-PEC	SHA-PEC	HA-PEC
Zeta potential (mV)	−58.7	−28.0	34.5	24.9	−5.7	29.5

Table 2
The cell number and differentiation of NHOst cultured on various PEC films after 1 week

Samples	The cell number (percent against control)	$\frac{\text{ALP activity}}{\text{The cell number}}$ (ratio)	$\frac{\text{Ca amount}}{\text{The cell number}}$ (μg/ratio)
Collagen-coated dish	100.0±17.0	1.00±0.15	3.4±0.5
S-PEC	82.2±6.1	0.98±0.11	10.7±3.6
CM-PEC	6.0±2.6*	0.05±0.08*	27.4±3.0*
P-PEC	130.4±6.3	0.02±0.01*	2.5±0.8
SHA-PEC	71.4±22.1	1.35±0.48	2.1±1.0
HA-PEC	8.1±3.0*	0.52±0.31	38.3±12.3*
Chitosan	79.5±25.0	0.93±0.13	2.7±2.0

*$p<0.01$ against collagen-coated dish.

with a carboxyl group, such as HA-PEC and CM-PEC, showed positive zeta potentials. In addition, P-PEC showed a positive potential less than that of HA-PEC. These data indicate that attachment of NHOst on surfaces with positive zeta potentials is reduced, suggesting the zeta potential of a PEC film partially controls cell attachment and morphology. Although all PEC were prepared by mixing anionic and cationic polysaccharides to neutralize their charge, zeta potential of each PEC film was ranged from −30 to 35 mV as shown in the table. This might indicate that not all anionic and cationic chemical groups were interacted to make PEC and their main chain composition and type of chemical groups may influence their side chain mobility, resulting in different surface zeta potential of each PEC. Details of surface properties of PEC films and their relationship to cell attachment will be reported in the near future.

After 1-week of incubation on various PEC films, the differentiation level of NHOst was estimated by measuring proliferation, alkaline phosphatase (ALP) activity and the amounts of calcium deposited. Table 2 shows the proliferation and ALP activity of NHOst cultured on various PEC films as well as the amounts of calcium deposited on the PEC. The proliferation of NHOst on the PEC is expressed as a percentage of proliferation of NHOst on a normal culture dish. The ALP activity was also calculated as a percentage of the control and normalized using the results of proliferation. In addition, the amount of calcium detected was normalized using the proliferation results as well. After a 1-week incubation, many dark spots, presumably calcium deposits, were observed on the collagen-coated dish and other PEC films (Fig. 2). When NHOst were cultured on CM-PEC or HA-PEC, it was observed that the NHOst aggregates were covered by the calcium deposits. It was reported that a surface with carboxyl group could induce calcium deposition after its incubation in simulated body fluid [27]. However, when the PEC were incubated in the medium without NHOst, no calcium deposition was detected. In addition, zeta potential estimation suggests less carboxyl groups are appeared on a surface of the PEC. These indicate that calcium deposition occurred only on aggregated NHOst but not on surfaces lacking NHOst. Therefore, normalization is necessary to estimate the capacity of PEC films to induce NHOst differentiation, although the raw values of deposited calcium or ALP activity are low. In fact, CM-PEC or HA-PEC films show a capacity to induce NHOst differentiation comparable to the collagen-coated dish and other PEC films, judging from the normalized values of deposited calcium shown in the table, even though the ratio of NHOst number on them was only 6–8% of that on a collagen-coated dish. Their ALP activities were, however, much lower than those on the collagen-coated dish. Incubation of the PEC films without NHOst for 1 week resulted in no calcium deposition, irrespective of their composition, suggesting that the PEC films themselves had no effect on calcium deposition. Thus, enhancement of calcium deposition on the PEC films may be ascribed to enhancement of NHOst functions related to their differentiation even though their ALP activity was suppressed. The reason for this inconsistency observed between calcium deposition and ALP activity must be investigated further.

When sulfated polysaccharides were used to prepare PEC films, proliferation of NHOst on the PEC films was 70–80% of that on a collagen-coated dish, and ALP activity was very similar to that on the collagen-coated dish. This suggests that sulfated polysaccharide PEC does not affect NHOst functions. Actually, there were no statistical differences in the amounts of calcium deposited between NHOst on the PEC and the collagen-coated dish although NHOst on S-PEC showed higher average calcium deposition. Thus, it is suggested that the PEC films made from sulfated polysaccharides are comparable substrates to a collagen-coated dish for cell culture. When compared to a normal culture dish, it has been reported that S-PEC can induce aggregation of cultured human fibroblasts and enhance their DNA synthesis in an earlier stage of cell culture by activation of the ERK pathway [28]. Since we used a collagen-coated dish as a control in this study, it is expected that the pathway of NHOst on the dish may be already activated through integrin molecules on the NHOst membrane. Therefore, the results in this study suggest the PEC from sulfated polysaccharides have a potential to proliferate and differentiate NHOst very similar to that of collagen.

To assess the effects of PEC films on cell function, gap junctional intercellular communication (GJIC), which is an important function of cells for maintenance of homeostasis [17], of NHOst on the films were measured. As shown in Fig. 4, GJIC of NHOst on PEC films did not show statistically significant differences compared to those grown on a collagen-coated dish. Although the GJIC of NHOst on CM-PEC showed a decrease after 1 day of incubation, it had recovered after 1 week. This result suggests that most PEC films have the potential to maintain homeostasis of attached cells although they showed different influences on the number and the differentiation of NHOst. On the other hand, NHOst on chitosan, which was used as the polycation for all PEC, showed suppression of GJIC after 1 week. This suggests that chitosan disturbs homeostasis maintenance of NHOst, but improve its biocompatibility by forming PEC films with other anionic polysaccharides. Therefore, PEC might be used as a biocompatible material for medical devices and tissue engineering scaffolds.

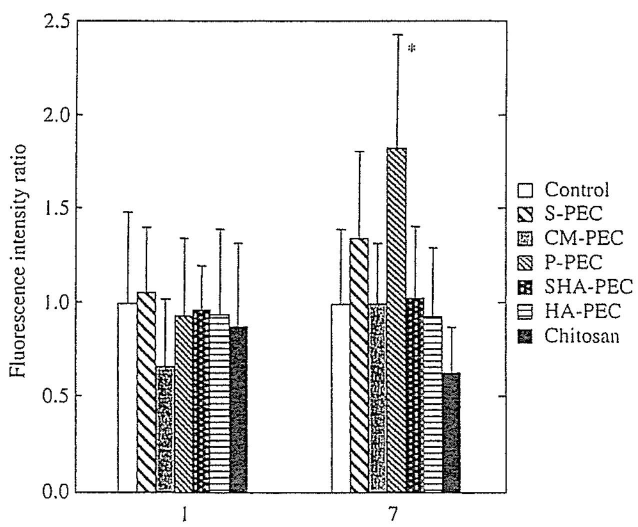

Fig. 4. Gap junctional intercellular communication activity of NHOst on various PEC films estimated by FRAP analysis technique. (* $p < 0.01$ against control).

4. Conclusion

PEC films composed of various polysaccharides were prepared, and their effects on NHOst functions were evaluated. Attachment, morphology, growth and differentiation of NHOst were influenced by the composition of the PEC on which they were grown. NHOst attachment decreased and their aggregates were observed on PEC prepared from polysaccharides containing a carboxyl group (CM- and HA-PEC). ALP activity of NHOst was suppressed on these PEC films although calcium deposition was observed more frequently than on other PEC films. In addition, these PEC films strongly suppressed proliferation of NHOst. PEC prepared from phosphated chitin and chitosan (P-PEC) showed low ALP activity and calcium deposition, although the number of NHOst was highest after 1-week incubation. These indicate unsuitability of these three PEC for usage in tissue engineering. On the other hand, NHOst adhered to and proliferated well on PEC films when sulfated polysaccharides were used as the polyanion (S- and SHA-PEC). Moreover, these PEC films showed almost the same suitability as the collagen-coated dish in all cell functions studied, indicating that these PEC films, especially S-PEC can be used as a scaffold for bone regeneration. Further studies, especially in vivo studies, are needed to clarify the usefulness of PEC films for tissue engineering.

Acknowledgements

This work was partially supported by Health and Labour Sciences Research Grants for Research on Advanced Medical Technology and Risk Analysis Research on Food and Pharmaceuticals by Ministry of Health, Labour and Welfare, Health and Labour Sciences Research Grants for Research on Health Sciences focusing on Drug Innovation by the Japan Health Sciences Foundation, and Grant-in-Aid for 21st Century COE Program "Advanced Fiber Engineering" and Grant-in-Aid for Scientific Research (B), 2002 (14350495) by Ministry of Education, Science, Sports and Culture.

References

[1] Adams JC, Watt FM. Regulation of development and differentiation by the extracellular matrix. Development 1993;117:1183–98.

[2] Peterson WJ, Tachiki KH, Yamaguchi DT. Extracellular matrix alters the relationship between thymidine incorporation and proliferation of MC3T3-E1 cells during osteogenesis in vitro. Cell Prolif 2002;35:9–22.

[3] Langer R, Vacanti JP. Tissue engineering. Science 1993;260:920–6.

[4] Mooney DJ, Mikos AG. Growing new organs. Sci Am 1999;280:38–43.

[5] Hori Y, Nakamura T, Matsumoto K, Kurokawa Y, Satomi S, Shimizu Y. Tissue engineering of the small intestine by acellular collagen sponge scaffold grafting. Int J Artif Organs 2001;24:50–4.

[6] Yamamoto M, Takahashi Y, Tabata Y. Controlled release by biodegradable hydrogels enhances the ectopic bone formation of bone morphogenetic protein. Biomaterials 2003;24:4375–83.

[7] Gamez E, Ikezaki K, Fukui M, Matsuda T. Photoconstructs of nerve guidance prosthesis using photoreactive gelatin as a scaffold. Cell Transplant 2003;12:481–90.

[8] Lavik E, Teng YD, Snyder E, Langer R. Seeding neural stem cells on scaffolds of PGA, PLA, and their co-polymers. Method Mol Biol 2002;198:89–97.

[9] Lieb E, Tessmar J, Hacker M, Fischbach C, Rose D, Blunk T, Mikos AG, Gopferich A, Schulz MB. Poly(D,L-lactic acid)-poly(ethylene glycol)-monomethyl ether diblock copolymers control adhesion and osteoblastic differentiation of marrow stromal cells. Tissue Eng 2003;9:71–84.

[10] Shin M, Ishii O, Sueda T, Vacanti JP. Contractile cardiac grafts using a novel nanofibrous mesh. Biomaterials 2004;25:3717–25.

[11] Alsberg E, Anderson KW, Albeiruti A, Rowley JA, Mooney DJ. Engineering growing tissues. Proc Nat Acad Sci 2002;99:12025–30.

[12] Chang CH, Liu HC, Lin CC, Chou CH, Lin FH. Gelatin-chondroitin-hyaluronan tri-copolymer scaffold for cartilage tissue engineering. Biomaterials 2003;24:4853–8.

[13] Tsuchida E, Abe K. Interactions between macromolecules in solution and intermacromolecular complexes. Adv Polym Sci 1982;45:1–119.

[14] Hamano T, Teramoto A, Iizuka E, Abe K. Effects of polyelectrolyte complex (PEC) on human periodontal ligament fibroblasts (HPLF) function. I. Three-dimensional structure of HPLF cultured PEC. J Biomed Mater Res 1998;41:257–69.

[15] Hamano T, Teramoto A, Iizuka E, Abe K. Effects of polyelectrolyte complex (PEC) on human periodontal ligament fibroblasts (HPLF) function. II. Enhancement of HPLF differentiation and aggregation on PEC by *L*-ascorbic acid and dexamethasone. J Biomed Mater Res 1998;41:270–7.

[16] Hamano T, Chiba D, Nakatsuka K, Nagahata M, Teramoto A, Kondo Y, Hachimori A, Abe K. Evaluation of a polyelectrolyte complex (PEC) composed of chitin derivatives and chitosan, which promotes the rat calvarial osteoblast differentiation. Polym Adv Technol 2002;13:46–53.

[17] Maio AD, Vaga VL, Contreras JE. Gap junctions, homeostasis, and injury. J Cell Physiol 2002;191:269–82.

[18] Tsuchiya T, Hata H, Nakamura A. Studies on the tumor-promoting activity of biomaterials: inhibition of metabolic cooperation by polyetherurethane and silicone. J Biomed Mater Res 1995;29:113–9.

[19] Tsuchiya T, Takahara A, Cooper SL, Nakamura A. Studies on the tumor-promoting activity of polyurethanes: depletion of inhibitory action of metabolic cooperation on the surface of a polyalkyleneurethane but not a polyetherurethane. J Biomed Mater Res 1995;29:835–41.

[20] Nakaoka R, Tsuchiya T, Sakaguchi K, Nakamura A. Studies on in vitro evaluation for the biocompatibility of various biomaterials: inhibitory activity of various kinds of polymer microspheres on metabolic cooperation. J Biomed Mater Res 2001:279–84.

[21] Nakaoka R, Tsuchiya T, Nakamura A. The inhibitory mechanism of gap junctional intercellular communication induced by polyethylene and the restorative effects by surface modification with various proteins. J Biomed Mater Res 2001;57:567–74.

[22] Nagahata M, Tsuchiya T, Ishiguro T, Matsuda N, Nakatsuchi Y, Teramoto A, Hachimori A, Abe K. A novel function of *N*-cadherin and connexin 43: marked enhancement of alkaline phosphotase activity in rat calvarial osteoblast exposed to sulfated hyaluronan. Biochem Biophys Res Commun 2004;315:603–11.

[23] Tamada Y, Ikada Y. Fibroblast growth on polymer surfaces and biosynthesis of collagen. J Biomed Mater Res 1994;28:783–9.

[24] Ohyama M, Suzuki N, Yamaguchi Y, Maeno M, Otsuka K, Ito K. Effect of enamel matrix derivative on the differentiation of C2C12 cells. J Periodontol 2002;73:543–50.

[25] Wade MH, Trosko JE, Schlindler M. A fluorescence photobleaching assay of gap junctional-mediated communication between human cells. Science 1986;232:525–8.

[26] Kato S, Akagi T, Sugimura K, Kishida A, Akashi M. Evaluation of biological responses to polymeric biomaterials by RT-PCR analysis IV: study of c-myc, c-fos and p53 mRNA expression. Biomaterials 2000;21:521–7.

[27] Tanahashi M, Matsuda T. Surface functional group dependence on apatite formation on self-assembled monolayers in a simulated body fluid. J Biomed Mater Res 1997;34:305–15.

[28] Matsuda N, Horikawa M, Yoshida M, Watanabe M, Nagahata M, Teramoto A, Abe K. Enhanced DNA synthesis accompanied by constitutive phosphorylation of the ERK pathway in human fibroblasts cultured on a polyelectrolyte complex. Biomaterials 2003;24:4771–6.

TISSUE ENGINEERING
Volume 11, Number 9/10, 2005

Enhancement of Gap Junctional Intercellular Communication of Normal Human Dermal Fibroblasts Cultured on Polystyrene Dishes Grafted with Poly-*N*-isopropylacrylamide

TSUTOMU NAGIRA, Ph.D.,[1,2] SUSAN BIJOO MATTHEW, Ph.D.,[1]
YOKO YAMAKOSHI, Ph.D.,[3] and TOSHIE TSUCHIYA, Ph.D.[1]

ABSTRACT

Technology developed to allow recovery of cells without enzyme treatment, involving a dish grafted with a thermoreactive polymer gel of poly-*N*-isopropylacrylamide (PIPAAm), was found to significantly enhance gap junctional intercellular communication (GJIC) in normal human dermal fibroblasts (NHDF cells). NHDF cells were cultured for 4 days on PIPAAm-grafted dishes irradiated with various doses of electron beams, and GJIC was assayed by the scrape-loading dye transfer method. The area of dye transfer was greater in the PIPAAm-grafted dishes than in the control culture dishes, indicating that the PIPAAm-grafted dishes enhanced the GJIC of NHDF cells. Connexin-43 (Cx43) expression was analyzed because Cx43 is considered to be a main component of the gap junctional channel. PIPAAm-grafted dishes irradiated with 100, 250, or 500 kGy of electron beams showed significantly enhanced expression of Cx43-NP, Cx43-P1, and especially Cx43-P2. Enhanced expression of Cx43-P2, a functional transmembrane protein, may be related to the promotion of GJIC. These results suggest that the PIPAAm-grafted dish not only enables the enzyme-free recovery of a cell monolayer for use in the construction of a three-dimensional artificial tissue, but also significantly contributes to the enhancement of GJIC, which may partly promote tissue strength on the surface of the PIPAAm-grafted dish.

INTRODUCTION

Gap junctions exist on the cell membrane and work as intercellular channels that allow the exchange of substances with molecular masses up to 1 kDa, such as ions, sugars, and amino acids, by the function called gap junctional intercellular communication (GJIC).[1–3] Gap junctions are constructed from transmembrane proteins, called connexins,[4,5] that form a hemichannel, called a connexon. GJIC is suggested to be well correlated with passage of metabolites,[6] cell proliferation,[7] and cell differentiation[8]; thus, enhancement of the function of the gap junction is supposed to be important in the differentiation of engineered tissue products, such as those involving heart cells.[9–11] Poly-*N*-isopropylacrylamide (PIPAAm)-grafted dishes, which were originally developed as a thermosensitive scaffold for cell culture, are useful to maintain the GJIC of tissues cultured on them because they do not require enzyme treatment, which destroys connexins.[12–14]

PIPAAm is a thermoresponsive polymer that has a low critical solution temperature of 32°C: hydrated PIPAAm

[1]Division of Medical Devices, National Institute of Health Sciences, Tokyo, Japan.
[2]Japan Association for the Advancement of Medical Equipment, Tokyo, Japan.
[3]Center for Polymers and Organic Solids, Department of Chemistry and Biochemistry, University of California, Santa Barbara, Santa Barbara, California.

has an extended chain conformation below 32°C and dehydrated PIPAAm has a collapsed chain conformation above 32°C.[15–27] This property of PIPAAm has been exploited in intelligent materials for drug delivery systems and chromatography technology.[16–23] The PIPAAm-grafted dish has been found to enable the recovery of cell monolayers easily without enzyme treatment because cells cannot adhere to a hydrophilic surface below 32°C.[24–26] Cell monolayers are the basic units used to construct three-dimensional tissues *in vitro*. Because a cell monolayer recovered without enzyme treatment maintains normal adhesive and junctional proteins, it can easily adhere to the other tissues or cell sheets to construct a three-dimensional artificial tissue.[27–29] Thus, the PIPAAm-grafted dish has the potential to enable the development of new techniques in tissue engineering.

Although the PIPAAm-grafted dish has made a new era in tissue engineering possible, its effects on connexin-43 (Cx43) expression and GJIC have not been studied well. These effects are important because Cx43 plays an important role in cell proliferation and cell differentiation.

In this study, GJIC and expression of Cx43 molecules were examined by scrape-loading dye transfer (SLDT) assay[30] and Western blotting, respectively, using NHDF cells cultured on PIPAAm-grafted dishes irradiated with various doses of electron beams in order to clarify the safety and appropriateness of this material for the culture of artificial cultured tissues.

MATERIALS AND METHODS

Materials

N-isopropylacrylamide monomer (NIPAAm) was purchased from Wako Pure Chemical Industries (Osaka, Japan). Isopropyl alcohol was obtained from Dojindo (Kumamoto, Japan), and Lucifer yellow dye was from Molecular Probes (Eugene, OR).

Cell culture

Normal human dermal fibroblasts (NHDF cells; Sanko Junyaku, Tokyo, Japan) were cultured in Dulbecco's modified Eagle's medium (GIBCO DMEM; Invitrogen, San Diego, CA), supplemented with 10% heat-inactivated fetal calf serum (FCS; Invitrogen) and antibiotics (penicillin [100 units/mL]-streptomycin [100 units/mL]) (Invitrogen) at 37°C. NHDF cells were maintained in a humidified atmosphere of 5% CO_2 and 95% air.

Preparation of PIPAAm-grafted culture dishes

One hundred microliters of 40% NIPAAm dissolved in isopropyl alcohol was added to 35-mm dishes and irradiated with various doses of electron beams (25, 100, 250, or 500 kGy), using an area electron beam-processing system (Nissin High Voltage, Kyoto, Japan). The PIPAAm-grafted dishes were then rinsed three times with ice-cold sterile water (2 ml) for 5 min, sealed, and dried under vacuum.

Cell morphology

NHDF cells were cultured on control and PIPAAm-grafted dishes. Confluent cells (after 4 days of culture) were fixed with formalin solution, stained with 3% Giemsa solution, and observed with an optical microscope.

Protein assay

The protein concentration of cells cultured on control and PIPAAm-grafted dishes was measured with a bicinchoninic acid (BCA) protein assay kit (Pierce Biotechnology, Rockford, IL). Ten-microliter cell samples were

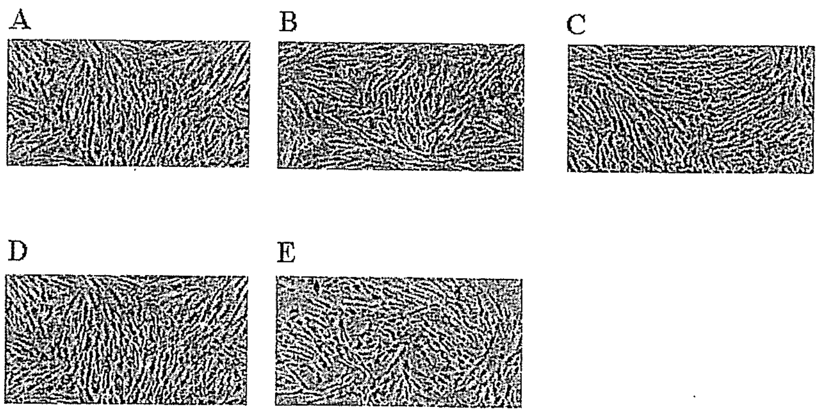

FIG. 1. Optical microscopy images of NHDF cells cultured on PIPAAm-grafted dishes. NHDF cells were cultured for 4 days on PIPAAm-grafted dishes prepared by irradiation with various doses of electron beams (0, 25, 100, 250, or 500 kGy). (A) Non-irradiated; (B) 25-kGy electron beam; (C) 100-kGy electron beam; (D) 250-kGy electron beam; (E) 500-kGy electron beam.

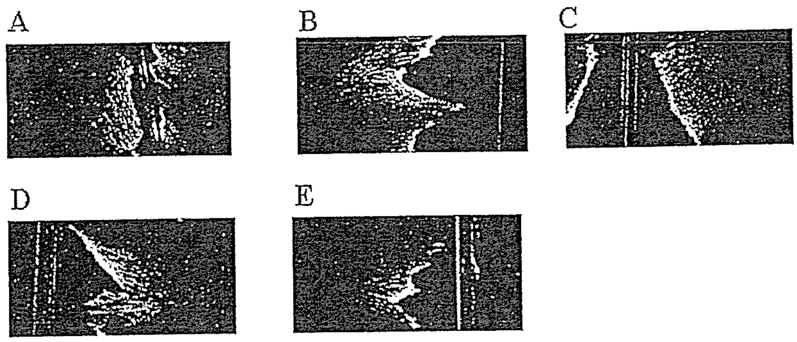

FIG. 2. Fluorescence of NHDF cells by SLDT assay. Transmission of Lucifer yellow into NHDF cells cultured on PIPAAm-grafted dishes irradiated with various doses of electron beams was detected 5 min after scrape-loading. (A) Nonirradiated; (B) 25-kGy electron beam; (C) 100-kGy electron beam; (D) 250-kGy electron beam; (E) 500-kGy electron beam.

added to 200 μL of the working solution and incubated at 37°C for 30 min in a 96-well plate. Absorbance was then measured at 562 nm in accordance with the manufacturer's protocols.

Scrape-loading dye transfer assay

NHDF cells were seeded on control and PIPAAm-grafted dishes at a density of 1×10^5 cells/mL and cultured for 4 days to form a confluent monolayer. Confluent NHDF cells were washed three times with phosphate-buffered saline containing Ca^{2+} and Mg^{2+} [PBS(+)], and the cell monolayer was scraped with a surgical blade. Fluorescent dye (Lucifer yellow; MW 457.2) at a concentration of 0.1% in PBS(+) was added.[30,31] Cells were exposed to the dye at 37°C for 5 min, and then the dye was discarded and the cells were washed four times with PBS(+). The distance that the dye had migrated was measured under a fluorescence microscope equipped with a type UFX-DXII CCD camera and super high-pressure mercury lamp power supply (Nikon, Tokyo, Japan). The dye migration was measured from the cut edge of the scrape to the edge of the dye front in the cells that were visually detectable.[30]

Western blotting

NHDF cells were cultured for 4 days. After being washed with ice-cold PBS(–) three times, the cells were lysed in 500 μL of lysis buffer (50 mM Tris-HCl [pH 6.8] containing 150 mM NaCl, 5 mM EDTA, 0.1 mM leupeptin, 1 mM phenylmethylsulfonyl fluoride, and 1% Nonidet P-40) for 30 min on ice with shaking. The cell lysates were centrifuged (10,000 rpm) at 4°C for 20 min, and the supernatants were collected. The protein concentrations of the lysates were determined by BCA assay.

Equivalent amounts of protein sample were applied to 12% sodium dodecyl sulfate (SDS)–polyacrylamide gels and then transferred to a nitrocellulose membrane at 120 V for 60 min. The membrane was blocked with Block Ace (Yukijirusi, Tokyo, Japan) overnight at 4°C. After being washed for 30 min in PBS with 0.05% Tween 20, the membrane was incubated for 2 h with anti-Cx43 polyclonal antibody [diluted 1:1000 in PBS(–) with 0.05% Tween 20; Zymed Laboratories, South San Francisco, CA], followed by incubation with horseradish peroxidase (HRP)-conjugated goat anti-rabbit IgG secondary antibody (diluted 1:5000; Zymed Laboratories). The image was visualized with an enhanced chemiluminescence (ECL) detection kit (Amersham Biosciences/GE Healthcare, Little Chalfont, UK).

Statistical analysis

Significant differences between groups were evaluated by Student *t* test. Mean differences were considered significant when $p < 0.05$.

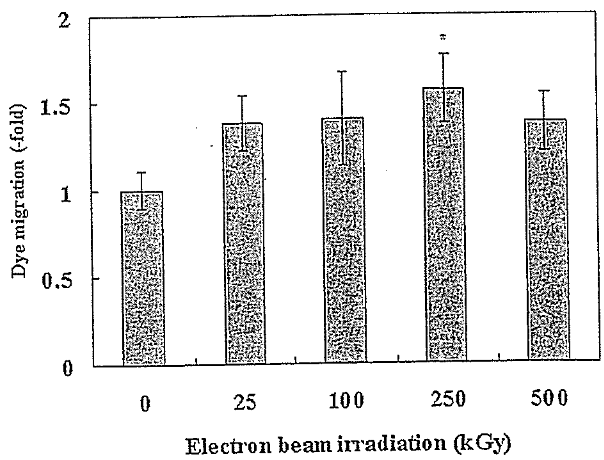

FIG. 3. Positive dye transfer in NHDF cells cultured on PIPAAm-grafted dishes. Transmission of Lucifer yellow was detected 5 min after scrape-loading in NHDF cells cultured on PIPAAm-grafted dishes irradiated with various electron beam doses (0, 25, 100, 250, or 500 kGy). Values represent means ± SD for three dishes. *Significant difference compared with control at $p < 0.05$ by *t* test.

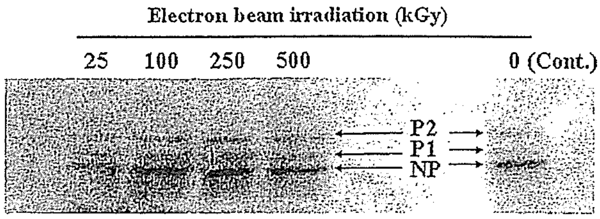

FIG. 4. Western blot of Cx43-NP, Cx43-P1, and Cx43-P2 expression; lysates of NHDF cells cultured on PIPAAm-grafted dishes irradiated with various doses of electron beams (0, 25, 100, 250, or 500 kGy) were applied to SDS–polyacrylamide gels. Fractionated proteins in the gels were transferred to nitrocellulose membrane and immunoblotted with anti-Cx43 polyclonal antibody as described in Material and Methods. Images of Cx43 on Western blot were captured with an Image scanner and analyzed with NIH Image software.

RESULTS

The appearance of NHDF cells grown on PIPAAm-grafted dishes irradiated with various doses of electron beams are shown in Fig. 1. No significant differences were observed by optical microscopy analysis between cells grown in dishes irradiated with various doses of electron beams. These results suggest that PIPAAm-grafted dishes are not toxic to NHDF cells.

The SLDT assay showed that dye migration in cells cultured on PIPAAm-grafted dishes irradiated with electron beams (25, 100, or 500 kGy) was enhanced by about 1.4-fold compared with that on control dishes. Interestingly, the dye migration in cells cultured on PIPAAm-grafted dishes irradiated with the 250-kGy electron beam was particularly enhanced, about 1.6 times higher than that on control dishes (Figs. 2 and 3). These results suggested that the GJIC of NHDF cells cultured on PIPAAm-grafted dishes was enhanced and that the GJIC on PIPAAm-grafted dishes irradiated with the 250-kGy electron beam was affected the most.

To further elucidate the effects of the PIPAAm grafting of culture dishes on GJIC, we analyzed the expression of Cx43, a transmembrane protein involved in GJIC. There are three forms of Cx43: Cx43-NP (nonphosphorylated Cx43), Cx43-P1 (monophosphorylated Cx43), and Cx43-P2 (another phosphorylated Cx43); Cx43-P2 is the most important and functional protein involved in GJIC. The results of Western blotting showed that the expression of Cx43-P1 and Cx43-P2 in NHDF cells cultured on PIPAAm-grafted dishes irradiated with 25, 100, 250, or 500 kGy of electron beams was considerably enhanced. Further, NHDF cells cultured on PIPAAm-grafted dishes irradiated with 100, 250, or 500 kGy of electron beams showed enhanced Cx43-NP expression (Figs. 4 and 5A). The Cx43-P2 expression of cells cultured on PIPAAm-grafted dishes irradiated with the 250-kGy electron beam dose showed the highest value, about 46% higher than that of control dishes. Cells cultured on PIPAAm-grafted dishes irradiated with electron beam doses of 25, 100, and 500 kGy were shown to have enhanced total Cx43 expression. Cells cultured on PIPAAm-grafted dishes irradiated with 100- and 250-kGy electron beam doses showed the highest total Cx43 expression, about 36.6% higher than that of control dish (Fig. 5B).

The Cx43-P2 expression of NHDF cells cultured on PIPAAm-grafted dishes irradiated with 25, 100, 250, and 500 kGy correlated well with GJIC ($R^2 = 0.9398$).

DISCUSSION

Thermoresponsive PIPAAm-grafted dishes irradiated with electron beams have been used to culture cell monolayers because the monolayers can be recovered without enzyme treatment, making PIPAAm a useful material for tissue engineering.

It has been reported that junctional proteins, cellular adherence proteins on the cell membrane, interact via

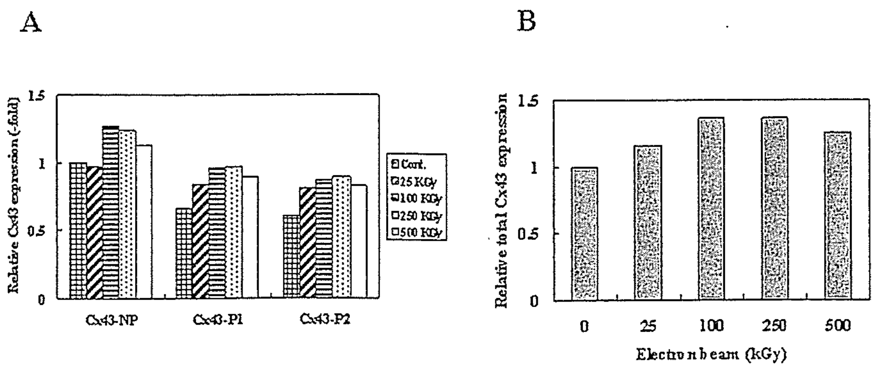

FIG. 5. Relative expression levels of Cx43-NP, Cx43-P1, and Cx43-P2 (A) and relative expression levels of total Cx43 (NP+P1+P2) (B) of NHDF cells cultured on PIPAAm-grafted dishes irradiated with various doses of electron beams (0, 25, 100, 250, or 500 kGy).

GJIC.[31] In this study, an SLDT assay demonstrated that dye migration in cultured NHDF cells was significantly enhanced in all PIPAAm-grafted dishes tested. Therefore, the chemical structure of the PIPAAm surface may stimulate junctional proteins on the cell membrane, and the stimulated junctional proteins may induce the enhancement of GJJIC.

Cx43 expression of NHDF cells cultured on PIPAAm-grafted dishes irradiated with a 250-kGy electron beam changed significantly. Structural differences in PIPAAm triggered by the 250-kGy electron beam induced Cx43 protein expression by NHDF cells, probably by affecting the gene expression of NHDF cells. Further, total Cx43 expression was shown to be enhanced in cells cultured on PIPAAm-grafted dishes irradiated with various doses of electron beams (25, 100, 250, or 500 kGy). Differences due to the electron beam dose should be studied further.

Although the mechanism involved was not determined, it has been reported that basic fibroblast growth factor (bFGF) and keratinocyte growth factor (KGF) enhance GJIC activity and the expression of Cx43.[32–35] If bFGF and KGF in FCS are adsorbed onto the PIPAAm surface, cells can efficiently access these growth factors from the PIPAAm surface, and GJIC may be enhanced. It is also reported that bFGF activates protein kinase A (PKA),[36] an important regulator of Cx43, promoting the phosphorylation of Cx43 and enhancing GJIC.[37] Therefore, bFGF adsorbed onto the PIPAAm surface may bind its receptor and induce the activation of PKA, resulting in an enhancement of GJIC on NHDF cells caused by the increase in Cx43-P2 band protein.

In the process of posttranslational change, Cx43-P2 becomes insoluble in Triton X-100.[38] Thus, not all Cx43-P2 may be included in the lysate, and some Cx43-P2 may have been included in the pellet. More Cx43-P2 may have existed than was detected in the present results obtained by Western blotting.

In this study, it was shown that the use of PIPAAm-grafted dishes irradiated with various doses of electron beams enhanced GJIC and Cx43 expression in cultured NHDF cells. This suggests that PIPAAm-grafted dishes may promote efficient tissue regeneration, because GJIC plays an important role in increasing tissue strength.[39]

ACKNOWLEDGMENTS

This work was supported in part by a Grant-in-Aid for Scientific Research on Advanced Medical Technology from the Ministry of Labor, Health, and Welfare, Japan and by a Grant-in-Aid from the Japan Human Sciences Foundation.

REFERENCES

1. Giaume, C., Tabernero, A., and Medina, J.M. Metabolic trafficking through astrocyte gap junctions. Glia **21,** 114, 1997.
2. Abdullah, K.M., Luthra, G., Bilski, J.J., Abdullah, S.A. Reynolds, L.P., Redmer, D.A., and Grazul-Bilska, A.T. Cell-to-cell communication and expression of gap junctional proteins in human diabetic and nondiabetic skin fibroblasts. Endocrine **10,** 35, 1999.
3. Grossman, H.B., Liebert, M., Lee, I.W., and Lee, S.W. Decreased connexin expression and intercellular communication in human bladder cancer cells. Cancer Res. **54,** 3062, 1994.
4. Vera, B., Sanchez-Abarca, L.I., Bolanos, J.P., and Medina, J.M. Inhibition of astrocyte gap junctional communication by ATP depletion is reversed by calcium sequestration. FEBS Lett. **392,** 225, 1996.
5. Bukauskas, F.F., Jordan, K., Bukauskiene, A., Bennett, M.V., Lampe, P.D., Laird, D.W., and Verselis, V.K. Clustering of connexin 43–enhanced green fluorescent protein gap junction channels and functional coupling in living cells. Proc. Natl. Acad. Sci. U.S.A. **97,** 2556, 2000.
6. Giaume, C., Tabernero, A., and Medina, J.M. Metabolic trafficking through astrocytic gap junctions. Glia **21,** 114, 1997.
7. Tabernero, A., Jimenez, C., Velasco, A., Giaume, C., and Medina, J.M. The enhancement of glucose uptake caused by the collapse of gap junction communication is due to an increase in astrocyte proliferation. J. Neurochem. **78,** 890, 2001.
8. Tsuchiya, T. A useful marker for evaluating tissue-engineered products: Gap-junctional communication for assessment of the tumor-promoting action and disruption of cell differentiation in tissue-engineered products. J. Biomater. Sci. Polym. Ed. **11,** 947, 2000.
9. Giaume, C., Marin, P., Cordier, J., Glowinski, J., and Premont, J. Adrenergic regulation of intercellular communications between cultured striatal astrocytes from the mouse. Proc. Natl. Acad. Sci. U.S.A. **88,** 5577, 1991.
10. Warn-Cramer, B.L., Cottrell, G.T., Burt, J.M., and Lau, A.F. Regulation of connexin-43 gap junctional intercellular communication by mitogen-activated protein kinases. J. Biol. Chem. **273,** 9188, 1998.
11. Shimizu, T., Yamato, M., Isoi, Y., Akutsu, T., Setomaru, T., Abe, K., Kikuchi, A., Umezu, M., and Okano, T. Fabrication of pulsatile cardiac tissue grafts using a novel 3-dimensional cell sheet manipulation technique and temperature-responsive cell culture surfaces. Circ. Res. **22,** e40, 2002.
12. Nandkumar, M.A., Yamato, M., Kushida, A., Konno, C., Hirose, M., Kikuchi, A., and Okano, T. Two-dimensional cell sheet manipulation of heterotypically co-cultured lung cells utilizing temperature-responsive culture dishes results in long-term maintenance of differentiated epithelial cell functions. Biomaterials **23,** 1121, 2002.
13. Kushida, A., Yamato, M., Kikuchi, A., and Okano, T. Two-dimensional manipulation of differentiated Madin–Darby canine kidney (MDCK) cell sheets: The noninvasive harvest from temperature-responsive culture dishes and transfer to other surfaces. J. Biomed. Mater. Res. **54,** 37, 2001.
14. Shimizu, T., Yamato, M., Akutsu, T., Shibata, T., Isoi, Y., Kikuchi, A., Umezu, M., and Okano, T. Electrically com-

municating three-dimensional cardiac tissue mimic fabricated by layered cultured cardiomyocyte sheets. J. Biomed. Mater. Res. **60,** 110, 2002.
15. Takezawa, T., Mori, Y., and Yoshizato, K. Cell culture on a thermo-responsive polymer surface. Biotechnology **8,** 854, 1990.
16. Chung, J.E., Yokoyama, M., Yamato, M., Aoyagi, T., Sakurai, Y., and Okano, T. Thermo-responsive drug delivery from polymeric micelles constructed using block copolymers of poly(*N*-isopropylacrylamide) and poly (butylmethacrylate). J. Control. Release **62,** 115, 1999.
17. Chung, J.E., Yokoyama, M., and Okano, T. Inner core segment design for drug delivery control of thermo-responsive polymeric micelles. J. Control. Release **65,** 93, 2000.
18. Kurisawa, M., Yokoyama, M., and Okano, T. Gene expression control by temperature with thermo-responsive polymeric gene carriers. J. Control. Release **69,** 127, 2000.
19. Kobayashi, J., Kikuchi, A., Sakai, K., and Okano, T. Aqueous chromatography utilizing pH-/temperature-responsive polymer stationary phases to separate ionic bioactive compounds. Anal. Chem. **73,** 2027, 2001.
20. Kikuchi, A., and Okano, T. Pulsatile drug release control using hydrogels. Adv. Drug Deliv. Rev. **54,** 53, 2002.
21. Kanazawa, H., Sunamoto, T., Ayano, E., Matsushima, Y., Kikuchi, A., and Okano, T. Temperature-responsive chromatography using poly (*N*-isopropylacrylamide) hydrogel-modified silica. Anal. Sci. **18,** 45, 2002.
22. Kobayashi, J., Kikuchi, A., Sakai, K., and Okano, T. Aqueous chromatography utilizing hydrophobicity-modified anionic temperature-responsive hydrogel for stationary phases. J. Chromatogr. A **958,** 109, 2002.
23. Yoshizako, K., Akiyama, Y., Yamanaka, H., Shinohara, Y., Hasegawa, Y., Carredano, E., Kikuchi, A., and Okano, T. Regulation of protein binding toward a ligand on chromatographic matrixes by masking and forced-releasing effects using thermoresponsive polymer. Anal. Chem. **74,** 4160, 2002.
24. Kikuchi, A., Okuhara, M., Karikusa, F., Sakurai, Y., and Okano, T. Two-dimensional manipulation of confluently cultured vascular endothelial cells using temperature-responsive poly(*N*-isopropylacrylamide)-grafted surfaces. J. Biomater. Sci. Polym. Ed. **9,** 1331, 1998.
25. Kushida, A, Yamato, M., Konno, C., Kikuchi, A., Sakurai, Y., and Okano, T. Temperature-responsive culture dishes allow nonenzymatic harvest of differentiated Madin–Darby canine kidney (MDCK) cell sheets. J. Biomed. Mater. Res. **51,** 216, 2000.
26. Shimizu, T., Yamato, M., Kikuchi, A., and Okano, T. Two-dimensional manipulation of cardiac myocyte sheets utilizing temperature-responsive culture dishes augments the pulsatile amplitude. Tissue Eng. **7,** 141, 2001.
27. Hirose, M., Yamato, M., Kwon, O.H., Harimoto, M., Kushida, A., Shimizu, T., Kikuchi, A., and Okano, T. Temperature-responsive surface for novel co-culture systems of hepatocytes with endothelial cells: 2-D patterned and double layered co-cultures. Yonsei Med. J. **41,** 803, 2000.
28. Yamato, M., Utsumi, M., Kushida, A, Konno, C., Kikuchi, A., and Okano, T. Thermo-responsive culture dishes allow the intact harvest of multilayered keratinocyte sheets without dispase by reducing temperature. Tissue Eng. **7,** 473, 2001.
29. Harimoto, M., Yamato, M., Hirose, M., Takahashi, C., Isoi, Y., Kikuchi, A., and Okano, T. Novel approach for achieving double-layered cell sheets co-culture: Overlaying endothelial cell sheets onto monolayer hepatocytes utilizing temperature-responsive culture dishes. J. Biomed. Mater. Res. **62,** 464, 2002.
30. el-Fouly, M.H, Trosko, J.E., and Chang, C.C. Scrape-loading and dye transfer: A rapid and simple technique to study gap junctional intercellular communication. Exp. Cell Res. **168,** 422, 1987.
31. Defamie, N., Mograbi, B., Roger, C., Cronier, L., Malassiné, A., Brucker-Davis, F., Fenichel, P., Segretain, D., and Pointis, G. Disruption of gap junctional intercellular communication by lindane is associated with aberrant localization of connexin43 and zonula occludens-1 in 42GPA9 Sertoli cells. Carcinogenesis **22,** 1537, 2001.
32. Pepper, M.S., and Meda, P. Basic fibroblast growth factor increases junctional communication and connexin 43 expression in microvascular endothelial cells. J. Cell. Physiol. **153,** 196, 1992.
33. Nadarajah, B., Makarenkova, H., Becker, D.L., Evans, W.H., and Parnavelas, J.G. Basic FGF increases communication between cells of the developing neocortex. J. Neurosci. **18,** 7881, 1998.
34. Park, J.U., and Tsuchiya, T. Increase in gap junctional intercellular communication by high molecular weight hyaluronic acid associated with fibroblast growth factor 2 and keratinocyte growth factor production in normal human dermal fibroblasts. Tissue Eng. **8,** 419, 2002.
35. Doble, B.W., and Kardami, E. Basic fibroblast growth factor stimulates connexin-43 expression and intercellular communication of cardiac fibroblast. Mol. Cell. Biochem. **143,** 81, 1995.
36. Pursiheimo, J.P., Jalkanen, M., Tasken, K., and Jaakkola, P. Involvement of protein kinase A in fibroblast growth factor-2-activated transcription. Proc. Natl. Acad. Sci. U.S.A. **97,** 168, 2000.
37. Faucheux, N., Zahm, J.M., Bonnet, N., Legeay, G., and Nagel, M.D. Gap junction communication between cells aggregated on a cellulose-coated polystyrene: Influence of connexin 43 phosphorylation. Biomaterials **25,** 2501, 2004.
38. Musil, L.C., and Goodenough, D.A. Biochemical analysis of connexin43 intracellular transport, phosphorylation, and assembly into gap junctional plaques. J. Cell Biol. **115,** 1357, 1991.
39. Gutstein, D.E., Morley, G.E., Tamaddon, H., Vaidya, D., Schneider, M.D., Chen, J., Chien, K.R., Stuhlman, H., and Fishman, G.I. Conduction slowing and sudden arrhythmic death in mice with cardiac-restricted inactivation of connexin43. Circ. Res. **88,** 333, 2001.

Address reprint requests to:
Toshie Tsuchiya, Ph.D.
Division of Medical Devices
National Institute of Health Sciences
1-18-1 Kamiyoga
Setagaya-ku, Tokyo 158-8501, Japan

E-mail: tsuchiya@nihs.go.jp

Hydroxy apatite microspheres enhance gap junctional intercellular communication of human osteoblasts composed of connexin 43 and 45

Ryusuke Nakaoka, Saifuddin Ahmed, Toshie Tsuchiya
Division of Medical Devices, National Institute of Health Sciences, 1-18-1 Kamiyoga, Setagaya-ku, Tokyo 158-8501, Japan

Received 26 September 2004; revised 14 December 2004; accepted 14 December 2004
Published online 17 June 2005 in Wiley InterScience (www.interscience.wiley.com). DOI: 10.1002/jbm.a.30328

Abstract: The aseptic loosening of artificial joints with associated periprosthetic bone resorption may be partly due to the suppression of osteoblast function to form new bone by wear debris from the joint. To assess the effect of wear debris on osteoblasts, effects of model wear debris on gap junctional intercellular communication (GJIC) of normal human osteoblasts were estimated. The GJIC activity of the osteoblasts after a 1-day incubation with the microspheres was similar to that of normal osteoblasts. However, hydroxy apatite particles, which have been reported to enhance the differentiation of osteoblasts in contact with them, enhanced the GJIC function of the osteoblasts. From RT-PCR studies, not only connexin 43 but also connexin 45 is suggested to play a role in the GJIC of the osteoblasts in an early stage of coculture with the microspheres, although it is still unclear how these connexins work and are regulated in the GJIC and differentiation. However, this study suggests that there is a relationship between the early levels of GJIC and the differentiation of the cells. Therefore, estimating the effect of biomaterials, even in the microsphere form, on the GJIC of model cells, with which the biomaterials may be in contact *in vivo*, can provide important information about their biocompatibility. © 2005 Wiley Periodicals, Inc. J Biomed Mater Res 74A: 181–186, 2005

Key words: gap junctional intercellular communication; human osteoblasts; microspheres; hydroxy apatite; connexin

INTRODUCTION

Biomaterials implanted into the harsh environment of the body cannot maintain their original shape, or even their desired function, sometimes resulting in undesirable side effects. One well-known example is the aseptic loosening of artificial joints observed in many patients who underwent a total joint replacement 5 to 25 years ago. It has already been reported that aseptic loosening with associated periprosthetic bone resorption is partly due to the activation of macrophages and osteoclasts by wear debris from the artificial joint.[1–14] Macrophages stimulated by wear debris *in vitro* release significant amounts of inflammatory mediators such as interleukin-1, interleukin-6, prostaglandin E2, collagenase, and tumor necrosis factor.[6–14] In addition, the biological effects of wear debris may depend on the type of material used as well as the shape, size, and amount of the debris.[4–11] Therefore, it is important to estimate the biocompatibility of biomaterials with not only their original shape but also possible transformed shapes after their usage.

During the last decade, we have been researching the inhibitory potential of many kinds of biomaterials on gap junctional intercellular communication (GJIC) as an index for their biocompatibility.[15–18] GJIC is a function that plays an important role in maintaining cell and tissue homeostasis by exchanging low molecular weight molecules, which results in regulating cell growth, development, and differentiation of cells.[19,20] Therefore, it is reasonable that disruption of this function is the cause of many kinds of diseases. In a previous report,[18] we examined the inhibitory activity of polymer microspheres, which were used as model wear debris from biomedical polymer *in vivo*, on the GJIC of rodent-derived fibroblasts. We concluded that estimating the inhibitory activity of the microspheres on the GJIC might be useful for considering their side effects in the body. In other words, it may be possible to predict whether wear debris causes aseptic loosening of artificial joints by estimating their effect on GJIC function.

No benefit of any kind will be received either directly or indirectly by the authors
Correspondence to: R. Nakaoka; e-mail: nakoaka@nihs.go.jp

However, it must be noted that the effects of the microspheres may be different when the effects on the GJIC of human-derived cells are estimated. Osteoblasts have been reported to communicate with one another via GJIC function, and the function is believed to be critical to the coordinated cell behavior necessary in bone tissue development.[21,22] Therefore, the question is raised whether wear debris has an inhibitory effect on the GJIC and the GJIC inhibition has a relation with the aseptic loosening of artificial joints. Because we have already observed some precoated polymer microspheres around 5 μm in diameter showed the potential to inhibit GJIC of fibroblasts contacting with them,[23] we estimated effects of various microspheres around 5 μm in diameter on GJIC function using normal human osteoblasts to discuss the relationship between the GJIC and the differentiation of osteoblasts. In this study, we employed fluorescence recovery after photobleaching (FRAP) analysis for estimating the GJIC function,[17] and assessed the potential effect of many kinds of microspheres on the GJIC.

MATERIALS AND METHODS

Microspheres

Monodispersed polystyrene (PS) microspheres (5 μm in diameter) were purchased from Japan Synthetic Rubber Co., Ltd. (Tokyo, Japan). Low-density polyethylene (PE) microspheres were generously supplied by Sumitomo Seika chemicals Co., Ltd. (Tokyo, Japan). Alumina (Al_2O_3) microspheres were obtained from the Association of Powder Process Industry and Engineering. Sintered hydroxy apatite microspheres (HA, 7.2 μm in diameter) were prepared and supplied by Ube Material Industries, Ltd. A Multisizer II (Coulter Electronics Inc., Hialeah, FL) was used to determine the average diameter of PE and alumina microspheres: 6.4 and 5.1 μm, respectively. Microspheres were sterilized by dispersing them in a 70% ethanol solution, followed by centrifugation in sterile conditions to remove the ethanol solution. The microspheres were dispersed in sterile methanol for cell differentiation tests at specified concentrations. The suspension of microspheres in methanol was added to 35-mm type I collagen-coated cell culture dishes (Asahi techno glass, Chiba, Japan), and the plates dried overnight at room temperature. The obtained microsphere-coated dishes (100 μg/dish) were subjected to the assays.

Cell culture

Normal human osteoblasts (NHOst) were purchased from BioWhitteker Inc. (Walkersville, MD). The standard culture of NHOst was performed using alpha minimum essential medium (Gibco) containing 20% fetal calf serum (FCS) (Kokusai Shiyaku Co., Ltd., Tokyo, Japan). The cells were maintained in incubators under standard conditions (37°C, 5%-CO_2-95%-air, saturated humidity). All assays were performed using alpha minimum essential medium containing 20% FCS, supplemented with 10 m*M* beta-glycerophosphate. NHOst (1 $\times 10^5$ cells/dish/2.5 mL medium) were cultured on microsphere-coated dishes for estimating the effect of the microspheres interacted from the bottom of the cells. To estimate the effect of microspheres on cells adhered to the culture plates, the NHOst cells were cultured with microsphere-containing medium (100 μg/2.5 mL medium) after they had adhered to the collagen-coated dishes. The test cells were cultured while changing the medium three times when the measurement of GJIC was performed after a 7-day incubation.

Measurement of GJIC activities

NHOst cultured with microspheres were subjected to fluorescence recovery after photobleaching (FRAP) analysis to estimate the inhibitory activity of these microspheres toward the GJIC. FRAP analysis was carried out according to an original procedure by Wade et al.,[24] with some modifications.[17] Briefly, NHOst were plated on microsphere-coated dishes and incubated for 1 or 7 days. After a wash with phosphate buffer saline (PBS) containing $MgCl_2$ and $CaCl_2$ [PBS(+)], the cells were incubated for 5 min at room temperature in PBS(+) containing 5,6-carboxyfluorescein diacetate (7 μg/mL, excitation 488 nm and emission 515 nm). After the washing off of excess extracellular dye with PBS(+), the cells in the test dishes in PBS(+) were subjected to the FRAP analysis. In the control experiment, cells were inoculated on an untreated glass bottom dish and treated with the same procedure as the tested cells. Cells in contact with test microspheres and at least two other cells were subjected to FRAP analysis under an Ultima-Z confocal microscope (Meridian Instrument, Okemos, MI) with a 10× objective lens at room temperature. The cells were photobleached with a 488-nm beam and the recovery of fluorescence intensity was subsequently monitored at 1-min intervals for a total period of 4 min. The data obtained from more than seven independent cells were expressed as the average of fluorescence recovery rate in comparison to the rate obtained from NHOst cultured without microspheres.

Effect of microspheres on calcium deposition by NHOst

The amount of calcium deposited during a 7-day incubation of the cells were evaluated as follows: NHOst were cocultured with either precoated or added microspheres in 24-well collagen-coated culture plates (Asahi techno glass, Chiba, Japan) for 1 week (2 $\times 10^4$ cells/20 μg microspheres/well/500 μL medium). After the cells were fixed in formaldehyde, 0.5 mL of 0.1 *M* HCl was added to each well after washing the cells with PBS. The amounts of calcium dissolved in HCl were estimated using a Calcium detecting kit (Calcium-C test Wako, Wako, Osaka, Japan) according to the manufacturer's direction.

RT-PCR for estimating expression of connexins

According to the method reported by Ichikawa et al.,[25] RT-PCR was performed to detect the expression of connexin mRNA in NHOst. After culturing NHOst with microspheres for a scheduled time, total RNA was extracted from the NHOst using TRIZOL® reagent (Invitrogen Corp., Carlsbad, CA) according to the manufacturer's instructions. After dissolving the RNA in diethylpyrocarbonate-treated water, the total RNA concentration was measured spectrophotometrically using Genequant (Amarsham Biosciences Corp., Piscataway, NJ). RNA samples were adjusted to a minimum concentration among collected samples in each experiment and reversibly transcribed to cDNA using Superscript™ II (Invitrogen Corp.). For PCR amplification of human connexin 45, Takara Ex-Taq™ (Takara Shuzo Co., Ltd., Shiga, Japan) was used with Ex-Taq™ buffer consisting of 20 pmol each of two human connexin-45 specific primers (forward 5'GTGGCAACTCCCTCTGTGAT3' and reverse 5'GGATCCTCAAGTTCCCTCCT3'). For PCR amplification of human connexin 26, 32, and 43, Takara LA-Taq™ (Takara Shuzo Co., Ltd.) was used with Ex-Taq™ buffer consisting of 6 pmol each of the human connexin-specific primers (for connexin 26, forward 5'ATGGATTGGGGCACGC3' and reverse 5'TTAAACTGGCTTTTTTGACTTCCC3'. For connexin 32, forward 5'ATGAACTGGACAGGTTTGTACACCTTGCTC3' and reverse 5'TCAGCAGGCCGAGCAGCGG3'. For connexin 43, forward 5'ATGGGTGACTGGAGCGCCTTAGGC3' and reverse 5'CTAGATCTCCAGGTCATCAGGCCG3'). The PCR profile for connexin 45 involved pretreatment at 95°C for 2 min, followed by 35 cycles of denaturation at 95°C for 45 s, annealing at 54°C for 45 s, and extension at 72°C for 90 s. The PCR profile for connexin 26, 32, and 43 (35 times) was as follows: pretreatment at 95°C for 2 min, denaturation at 95°C for 30 s, annealing at 54°C for 30 s, and extension at 72°C for 120 s. Reaction products were analyzed by electrophoresis in 1.5% (w/v) agarose gel, followed by staining of the products by SYBR® Green I (Takara Shuzo Co., Ltd.) and detection of a 566-bp (connexin 45), 671-bp (connexin 26), 852-bp (connexin 32), and 1149-bp (connexin 43) band, respectively. For the standardization of connexin cDNA, PCR amplification of glyceraldehyde-3-phosphate dehydrogenase (GAPDH) mRNA in each sample was performed using GAPDH-specific primers (forward 5'CCCATCACCATCTTCCAGGAGCGAGA3' and reverse 5'TAAGTAGGACAACAAGGAGGTCGTGACGACGC3'; product size 578-bp). All reactions included negative controls without cDNA.

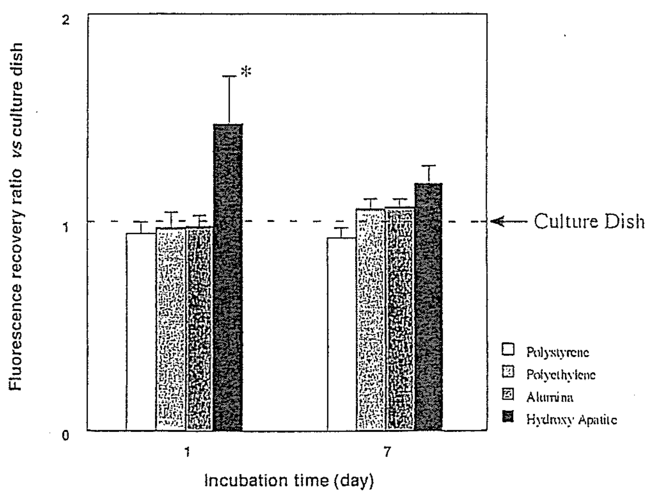

Figure 1. Effect of precoated microspheres on gap junctional intercellular communication of NHOst estimated from fluorescence recovery rates of target cells. The recovery rates of the cells on untreated culture dishes on days 1 and 7 were used as standards of all obtained data, respectively. (*$p < 0.01$ against culture dish).

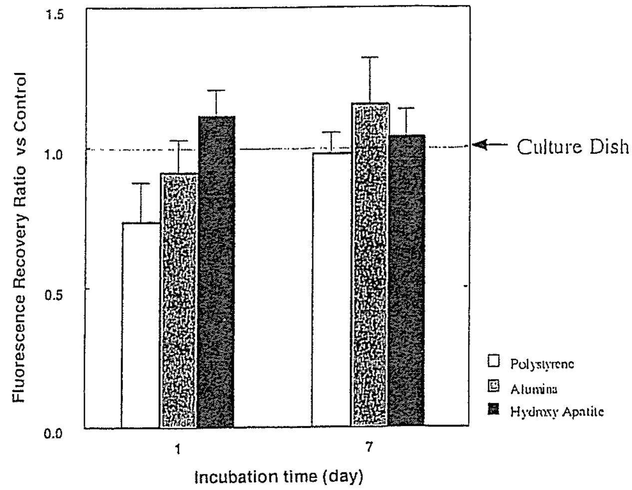

Figure 2. Effect of added microspheres on gap junctional intercellular communication of NHOst estimated from fluorescence recovery rates of target cells. The recovery rates of the cells on untreated culture dishes on days 1 and 7 were used as standards of all obtained data, respectively.

Statistical analysis

All data were expressed as the mean value ± the standard error of the means of the obtained data and treated statistically with Student's t test.

RESULTS

Figure 1 shows effects of various microspheres on GJIC of NHOst in contact with the microspheres for 1 and 7 days. The microspheres were precoated on 35-mm culture dishes before cell seeding. When the NHOst were cultured with precoated PS, PE, and alumina microspheres, their GJIC level was similar to that in NHOst cultured on a normal culture dish. On the other hand, the GJIC level was 1.5 times that of NHOst on the normal dish when they were cultured with precoated hydroxy apatite microspheres. After 7 days, the GJIC of NHOst in contact with microspheres became similar to that of normal NHOst, irrespective of the type of microsphere. The change in GJIC of NHOst in contact with added microspheres is shown in Figure 2. As seen in Figure 1, hy-

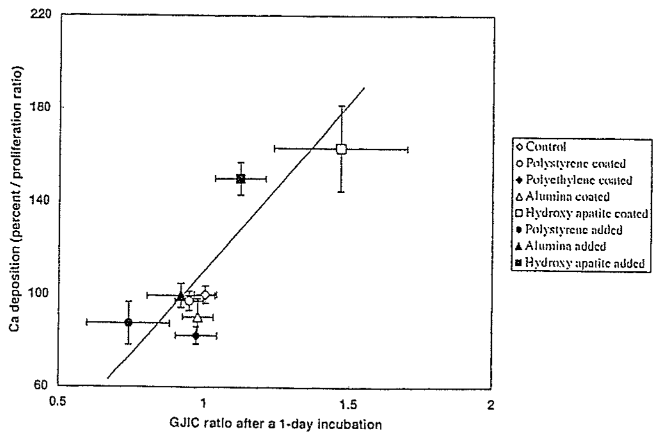

Figure 3. Relationship between GJIC on day 1 and calcium deposition ratio after 7-day coculture of NHOst with various microspheres ($r^2 = 0.74$).

droxy apatite microspheres enhanced their GJIC after a 1-day culture compared to cells on a normal plate. The degree of enhancement of GJIC is, however, smaller than that seen in NHOst in Figure 1, and no significant difference was observed between NHOst in contact with the hydroxy apatite microspheres and those cultured without microspheres. In addition, Figure 2 indicates that addition of PS microspheres into a culture of NHOst inhibited GJIC.

To consider the effects of tested microspheres on not only GJIC but also the differentiation of NHOst, changes in the amount of calcium deposited after a 1-week coculture of NHOst with various microspheres were estimated. From Figure 3, it is suggested that there is the possible relation between the GJIC of NHOst cocultured with microspheres for 1 day and

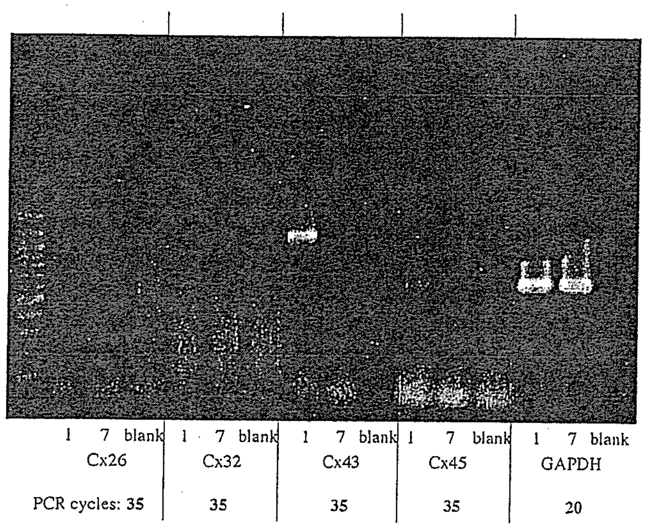

Figure 4. Expression of mRNA of various connexins (Cx) in NHOst cultured for 1 and 7 days. The number of NHOst cultured on 35-mm collagen-coated culture dishes was 2 × 10^5. RT-PCR cycles of each lane are expressed at the bottom of the figure.

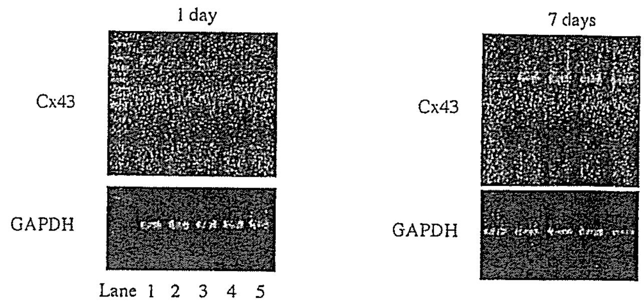

Figure 5. Expression of connexin 43 (Cx 43) mRNA in NHOst cultured with various precoated microspheres. The number of PCR cycles for connexin 43 and GAPDH is 35 and 20, respectively. Lane 1: without microspheres; lane 2: with PS microspheres; lane 3: with PE microspheres; lane 4: with alumina microspheres; lane 5: with HA microspheres.

the amount of calcium deposited after a 1-week coculture with the same microspheres.

To clarify which connexins exist in NHOst, we performed RT-PCR to detect mRNA of connexin 26, 32, 43, and 45 in NHOst cultured on a normal culture dish. Figure 4 shows the result of RT-PCR to amplify the mRNA from whole RNA collected from NHOst cultured for 1 and 7 days. As shown in the figure, only connexin 43 and 45 were detected in NHOst. When cells were cultured for 7 days, connexin 43 was detected at a lower level than that detected after the 1-day culture, while connexin 45 was not detected.

Figures 5 and 6 show the results of RT-PCR to amplify mRNA of connexin 43 and 45 in NHOst cultured with various precoated microspheres. The NHOst cultured with microspheres did not express mRNA of connexin 43, except those with PE microspheres. After 7 days, the expression was suppressed in the normal NHOst while the expression was observed in NHOst cultured with microspheres, irrespective of kind of the microsphere. On the other hand, mRNA expression of connexin 45 was suppressed after a 1-day culture of NHOst only with alumina microspheres, followed by a decrease in expression of the mRNA after their 7-day culture.

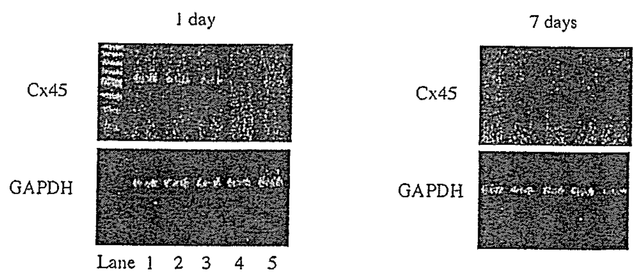

Figure 6. Expression of connexin 45 (Cx 45) mRNA in NHOst cultured with various precoated microspheres. The number of PCR cycles for connexin 45 and GAPDH is 40 and 20, respectively. Lane 1: without microspheres; lane 2: with PS microspheres; lane 3: with PE microspheres; lane 4: with alumina microspheres; lane 5: with HA microspheres.